

Development of Scalable Coding of Encrypted Images Using Modified Absolute Moment Block Truncation Code

Pankiraj Jeya Bright (✉ jeyabright@gmail.com)

Kalasalingam Academy of Research and Education <https://orcid.org/0000-0002-9246-5301>

Vishnuvarthanan Govindaraj

Kalasalingam University: Kalasalingam Academy of Research and Education

Yu-Dong Zhang

University of Leicester

Pallikonda Rajasekaran

Kalasalingam University: Kalasalingam Academy of Research and Education

Anisha Milton

Kalasalingam University: Kalasalingam Academy of Research and Education

Arunprasath Thiagarajan

Kalasalingam University: Kalasalingam Academy of Research and Education

Research

Keywords: Scalable Coding on Encrypted Image, Image Decryption, Image Reconstruction, Secured Signal Processing, Modified Absolute Moment Block Truncation Code, Image Encryption

Posted Date: January 3rd, 2022

DOI: <https://doi.org/10.21203/rs.3.rs-1205275/v1>

License: © ⓘ This work is licensed under a Creative Commons Attribution 4.0 International License.

[Read Full License](#)

Development of Scalable Coding of Encrypted Images Using Modified Absolute Moment Block Truncation Code

Jeya Bright Pankiraj^{1*}, Vishnuvarthanan Govindaraj², Yudong Zhang³, Pallikonda Rajasekaran Murugan⁴, Anisha Milton⁵, Arunprasath Thiagarajan⁶

^{1,4}Department of ECE, Kalasalingam Academy of Research and Education, Srivilliputhur, India

^{2,5,6}Department of BME, Kalasalingam Academy of Research and Education, Srivilliputhur, India

³F26, Informatics Building, School of Informatics, University of Leicester, University Road, Leicester, UK

*Correspondence: jeyabright@gmail.com

Abstract—Many researchers worked on scalable coding for unencrypted images, and there is more space for research in scalable coding for encrypted images. This paper proposes a novel method of scalable coding for encrypted images, especially for lossy compression images using the Modified Absolute Moment Block Truncation Code (MAMBTC) technique. The given input image is compressed using MAMBTC and then encrypted using a Pseudo-Random Number (PRNG) at the encryption phase. The PRNG is shared between the encoder and the decoder. At the decryption phase, the compressed pixel value is obtained by decryption using the PRNG and then reconstructed using MAMBTC, scaled by scaling factor 2 and Bilinear Interpolation Technique to obtain the original image. MAMBTC gives better image quality than Block Truncation Code (BTC), a higher PSNR of 36.32 dB, and a Compression ratio of 1.09, which makes the proposed system ready for the signal processing community/applications.

Keywords— Scalable Coding on Encrypted Image, Image Decryption, Image Reconstruction, Secured Signal Processing, Modified Absolute Moment Block Truncation Code, Image Encryption

1. Introduction

In today's technology, scalability is essentially required for transmission and reception of data, especially in the signal processing community, and therefore it is an essential area of

29 research. The Secured Signal Processing (SSP) for encrypted signals is performed on [1], and
30 Discrete Fourier Transform is implemented on [2] by using homomorphic properties. In [3],
31 the privacy problem is studied for adaptive filtering, and the same was analyzed for the
32 reduction of expansion factor in [4] for SSP in the encrypted domain. In [5], the digital
33 watermarking technique is proposed, and the enciphering rate is low, which is overcome by
34 using the fingerprinting technique in [6].

35 Nowadays, the usage of image data is larger, which has increased storage space and
36 bandwidth. It makes the transmission process costlier. Therefore, reducing storage space,
37 bandwidth and transmission costs are essential for the SSP on the encrypted domain. The
38 signals are first compressed and then encrypted, which is the traditional way of transmitting
39 data, but it is reversed in [7],[8],[9],[10] and [11].

40 Scalability is mostly preferred for many applications. Rate Scalability occurs when the
41 bit-stream is extracted at the desired rate from the decoder for lossy image, and higher bit rates
42 can be decoded until a perfect image is reconstructed. Resolution Scalability can be improvised
43 when a lower resolution of the lossy image is extracted from the decoder, and higher resolution
44 is achieved until the original image is reconstructed without loss. In [12] and [13], scalable
45 coding is carried out on unencrypted signals. The first work to report on scalable coding for
46 encrypted images is [14], where Hadamard transform is used for image compression, the
47 pseudo-random number is used for image encryption and image decryption, and scaling is done
48 by scaling factor 2. Later, bilinear interpolation technique is used for image reconstruction.

49 In this paper, the authors propose a novel method of scalable coding on encrypted
50 images using Modified Absolute Moment Block Truncation Code (MAMBTC) Technique. In
51 [15], the BTC technique was introduced in 1979. BTC works with two-level quantizers in
52 which the mean is used as a threshold value, and the original content is reconstructed using the

53 mean and variance value. In [16], the Absolute Moment Block Truncation Code (AMBTC)
54 technique was introduced in the year 1984, and AMBTC works with two-level quantizers in
55 which the mean is used as a threshold value. The original image is reconstructed using high
56 range and low range values. AMBTC technique is very attractive to many applications, such
57 as internet video with software-only codecs, digital cameras and printers that require only
58 moderate data rates. The advantage of the AMBTC technique was, the demand for storage
59 space is decreased and also it lends itself very nicely to parallel processing. In [17], scalable
60 coding is carried out by BTC for encrypted images. The principal content is compressed by
61 BTC, encrypted by PRNG and transmitted. It is further decrypted at the decoder, and the
62 principal content is reconstructed by applying techniques, such as BTC, scaled by scaling factor
63 2 and Bilinear Interpolation Technique. In this paper, the principal content is compressed by
64 MAMBTC and then encrypted using the PRNG, and finally, it is transmitted. The PRNG is
65 shared between encoder and decoder. The transmitted value is decrypted by PRNG on the
66 decoder, and the original image is reconstructed using the MAMBTC, scaled by scaling factor
67 2 and Bilinear Interpolation technique. The MAMBTC gives higher Peak Signal to Noise Ratio
68 (PSNR), better Compression Ratio (CR), and reduced Mean Squared Error (MSE), Bit Rate
69 (BR) than the existing techniques.

70 **2. Related Works**

71 *2.1.1 Scalable Coding of Encrypted Images using Hadamard Transform*

72 In [14], the raw image is encrypted by adding a pseudo-random number generated value
73 (PRNG), where the PRNG acts as a secret key. Then the encrypted image is divided into rough
74 content and detailed content. The rough content is rounded and quantized while detailed
75 content is taken Hadamard transform, and both encoded bits are transmitted by the encoder as
76 bit-streams. The bit-stream and secret key are shared with the decoder. At the decoder, rough

77 content is decrypted by subtracting it with the secret key, and the obtained value is kept
78 separately. The rough content value is taken bilinear transform to the original image size, and
79 after rounding and quantization, Hadamard transform is applied and resized to the detailed
80 content matrix size. Finally, the input image size is reconstructed by combining rough and
81 detailed content. However, the reconstructed image quality is with lower PSNR, lower CR, and
82 increased BR.

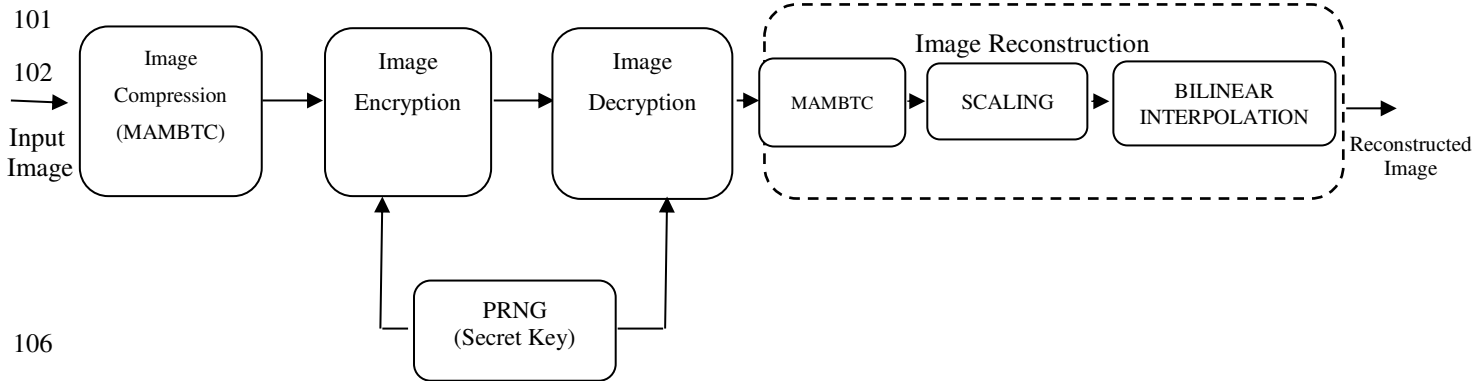
83 *2.1.2 Scalable Coding using BTC*

84 In [17], the authors have introduced the scalable coding of encrypted images using
85 BTC. In this, the principal content is compressed by BTC. It is then encrypted by PRNG, and
86 the same will be shared between encoder and decoder. The encoded bit-stream is transmitted.
87 In the decoding process, they first decrypt the transmitted image, and they reconstruct the
88 principal content by using techniques, such as BTC, scaling factor as 2, and bilinear
89 interpolation technique. This technique gives lower PSNR, lower CR, and higher MSE, and a
90 higher BR. We can achieve improved PSNR and CR values, and reduced MSE and BR by
91 using the developed MAMBTC technique.

92 **3. Proposed Method**

93 Fig.1 shows the proposed system. MAMBTC technique is used to compress the input
94 gray level pixel value. Then pseudo-random numbers (PRNG) are generated and added with
95 compressed pixel values to get the encrypted output. The PRNG is shared between encoder and
96 decoder. The transmitted bit stream is decrypted at the receiver side using the PRNG. Then the
97 principal content is reconstructed by MAMBTC and scaling technique. The reconstructed
98 content has better image quality, higher resolution, higher CR, lesser MSE, reduced BR, and
99 higher PSNR than the conventional BTC.

100



108 **Fig.1** Proposed System

109 3.1 Image Encoding Process

110 3.1.1 Image Compression

111 The first novelty introduced is the threshold value (T_{th}). The uncompressed input image

112 is gray in color. The input pixel values are within $[0, 255]$, and it will be in the form of a $B1 * B2$

113 matrix, where $B1$ is the row size, and $B2$ is the column size. The MAMBTC technique is

114 applied to the input image to get a compressed pixel value. It is then encrypted by adding the

115 compressed pixel value with the PRNG. The proposed MAMBTC algorithm steps are as

116 follow,

117 Step1: - The uncompressed input gray level image of size $512 * 512$ is divided into non-

118 overlapping blocks having size $B1 * B2$, where $B1$ and $B2$ values are taken as 4.

119 Step 2: - Each block is quantized to obtain the mean value. The mean (\bar{x}) is calculated using

120 equation (1), and these values are different for each block.

$$121 \bar{x} = \frac{1}{n} \sum_{i=1}^n x_i \quad (1)$$

122 Step 3: - The higher range and lower range values of each non-overlapping block are calculated,
 123 which are termed as quantizers of MAMBTC. The higher range (x_{HV}) value is calculated by
 124 taking the gray level value, which is greater than or equal to the mean value (\bar{x}) of the block as
 125 given in equation (2), where K represents the pixels whose gray level value is greater or equal
 126 than mean value (\bar{x}). The lower range (x_{LV}) value is calculated by taking the gray level value
 127 whose values are lesser than the mean value (\bar{x}) of the block as given by equation (3), which
 128 is expressed in scalar form.

$$129 \quad x_{HV} = \frac{1}{K} \sum_{x_i \geq \bar{x}} x_i \quad (2)$$

$$130 \quad x_{LV} = \frac{1}{16-K} \sum_{x_i < \bar{x}} x_i \quad (3)$$

131

132 Step 4:- The threshold value (T_{th}) is calculated by adding mean (\bar{x}), higher range (x_{HV}) value
 133 and lower range (x_{LV}) value and then divided by 3 for each non-overlapping block. It is given
 134 in equation (4) as:

135

$$136 \quad T_{th} = \frac{\bar{x} + x_{HV} + x_{LV}}{3} \quad (4)$$

137 Step 5:- The binary block ($c(i, j)$) is constructed by comparing each gray level value with the
 138 threshold value (T_{th}). The gray level values in the block having greater or equal than the
 139 threshold value is replaced by value "1" in the binary block, and those gray level having less
 140 than the threshold value is replaced by value "0" in the binary block. It is given by equation (5)
 141 as:

$$142 \quad c(i, j) = \begin{cases} 1 & x_i \geq T_{th} \\ 0 & x_i < T_{th} \end{cases} \quad (5)$$

143 This process reduces each block to a bit plane. Each non-overlapping block has a higher
 144 range value and lower range value meant to be shared to the receiver side, and they will be the
 145 same as higher range and lower range values for that block during reconstruction. Thus, the
 146 input image is compressed using MAMBTC.

147 3.1.2 Image Encryption

148 The second novelty is introduced in this by encrypting the MAMBTC compressed
 149 image. The bit amount for the compressed image is $8N$. The pseudo-random number (PRNG)
 150 of values between 0 and 255 for the size B_1*B_2 are produced by the pseudo-random number
 151 generator, and the pseudo-random bit sequence length is $8N$. Let $pr(i, j)$ be the PRNG value.
 152 The PRNG is shared with the decoder too. The encrypted pixel value is obtained by adding a
 153 compressed pixel value of size B_1*B_2 with the PRNG of size B_1*B_2 , and then masked by
 154 modulo 256. It is given as:

$$155 \quad en(i, j) = mod[(c(i, j) + pr(i, j)), 256] \quad (6)$$

$$156 \quad 1 \leq i \leq B_1, 1 \leq j \leq B_2$$

157 Where, $c(i, j)$ is the compressed image value, $pr(i, j)$ is the secret key, and $en(i, j)$ is the
 158 encrypted pixel value. The original image is shown in Fig. 2, and its encrypted image is shown
 159 in Fig.3. The image encryption algorithm used is semantically secure against any Probability
 160 Polynomial Time (PPT) adversary. The block is sent along with the secret key (PRNG) and
 161 also with values of higher range (X_{HV}) and lower range (X_{LV}).



Fig. 2 Original Image

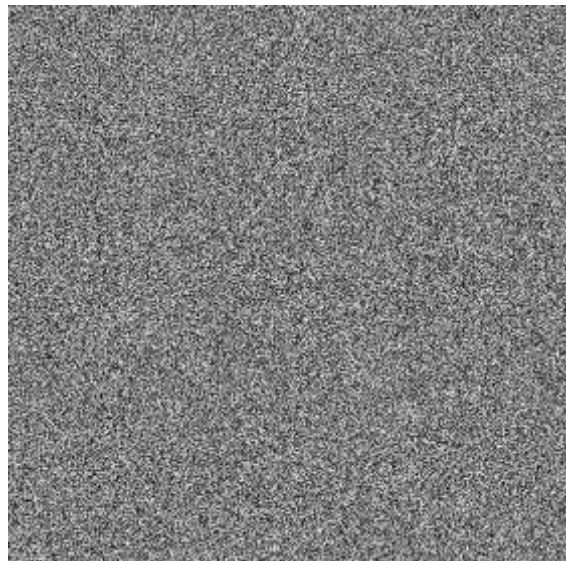


Fig. 3 Encrypted Image

162
163

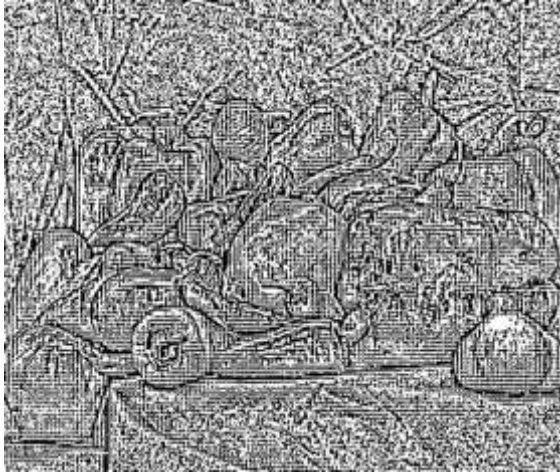
164 3.2 Image Decoding Process

165 3.2.1 Image Decryption

166 The secret key (PRNG) is received at the receiver. The decrypted image is obtained by
167 subtracting the transmitted encoded image with a secret key masked with the modulo-256
168 operation. The formula used is:

$$169 \quad de(i, j) = \text{mod}[(en(i, j) - pr(i, j)), 256] \quad (7)$$

170 Where $en(i, j)$ represents the transmitted encrypted image, $pr(i, j)$ represents the PRNG, and
171 $de(i, j)$ represents the compressed bit plane transmitted. The $de(i, j)$ contains two quantized
172 values, namely “0” and “1”. The decrypted image is shown in Fig. 4.



173
174 **Fig. 4** Decrypted Image



Fig. 5 Reconstructed Image

175 *3.2.2 Image Reconstruction*

176 The third novelty introduced in this paper is by having to scale on the MAMBTC
177 reconstructed image first, and then the original content is reconstructed by using the popular
178 scaling technique, namely Bilinear Interpolation Technique. The image reconstruction process
179 is in three stages. Firstly, by using the MAMBTC technique, the receiver side receives the high
180 range value and low range value transmitted by the encoder. The original content is
181 reconstructed by replacing the quantized value “1” in the decrypted compress bit plane by
182 higher range (X_{HV}) value and “0” by lower range (X_{LV}) value. It is given as:

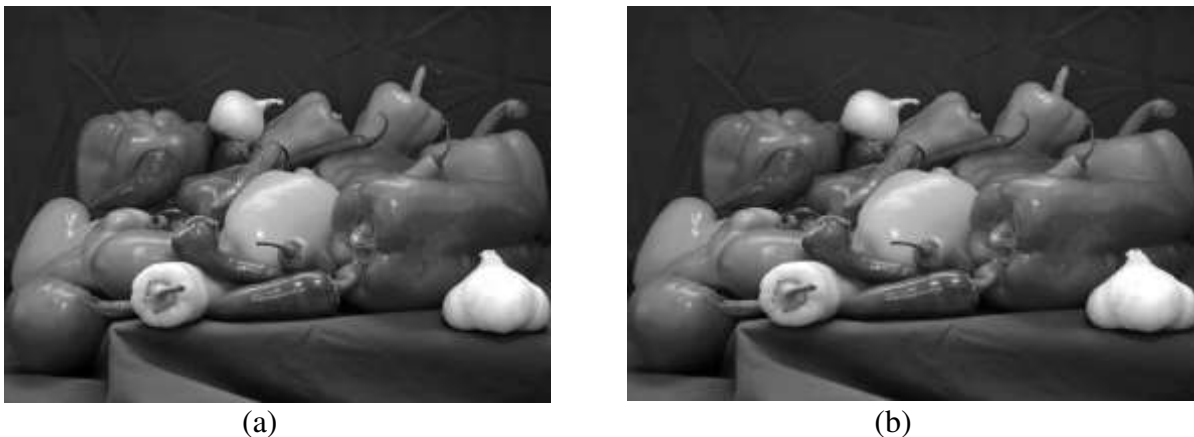
183
$$re(i,j) = \begin{cases} X_{HV}, & de(i,j) = 1 \\ X_{LV}, & de(i,j) = 0 \end{cases} \quad (8)$$

184 Accordingly, $re(i,j)$ gives the reconstructed image using MAMBTC. Secondly, it is
185 scaled by scaling factor 2, and finally, the original image size is reconstructed using Bilinear
186 Interpolation Technique. The reconstructed image is shown in Fig. 5.

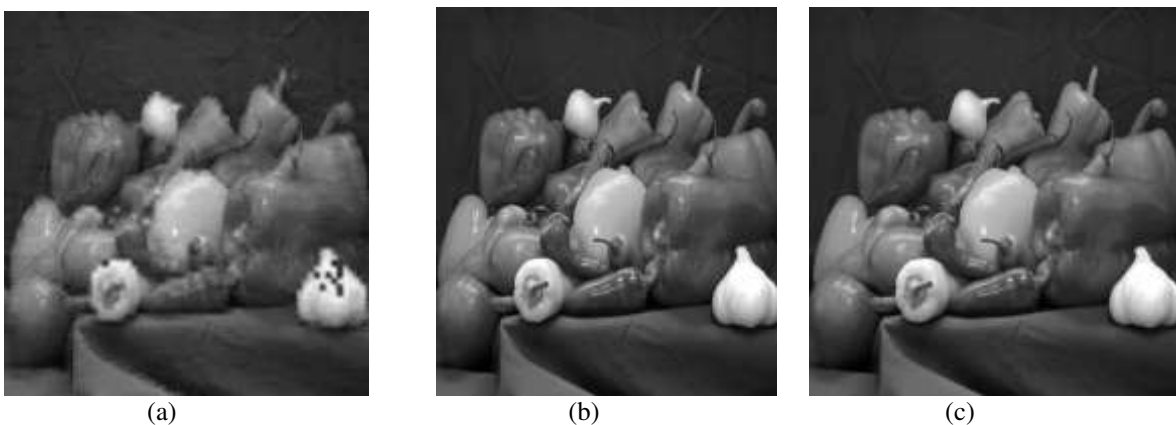
187 **4. Experimental Results and Discussion**

188 *4.1 Reconstructed Image*

189 The comparison between the original and reconstructed images is shown in Fig.6. The
 190 reconstructed image obtained has higher quality, and it reflects equivalent to the original image.
 191 The comparison between the reconstructed images using MAMBTC, BTC and Hadamard
 192 transform techniques is shown in Fig.7. It clearly shows that the quality of the reconstructed
 193 image using MAMBTC is much better than BTC and Hadamard transform in terms of PSNR,
 194 wPSNR, MSE, wMSE and compression ratio.



195
 196
 197 **Fig. 6** Comparison between the original image and the reconstructed image (a). Original Image (b).
 198 Reconstructed Image
 199



200
 201
 202 **Fig. 7** Comparison between reconstructed images using MAMBTC, BTC and Hadamard Transform techniques
 203 (a) Hadamard (b) BTC (c) MAMBTC
 204

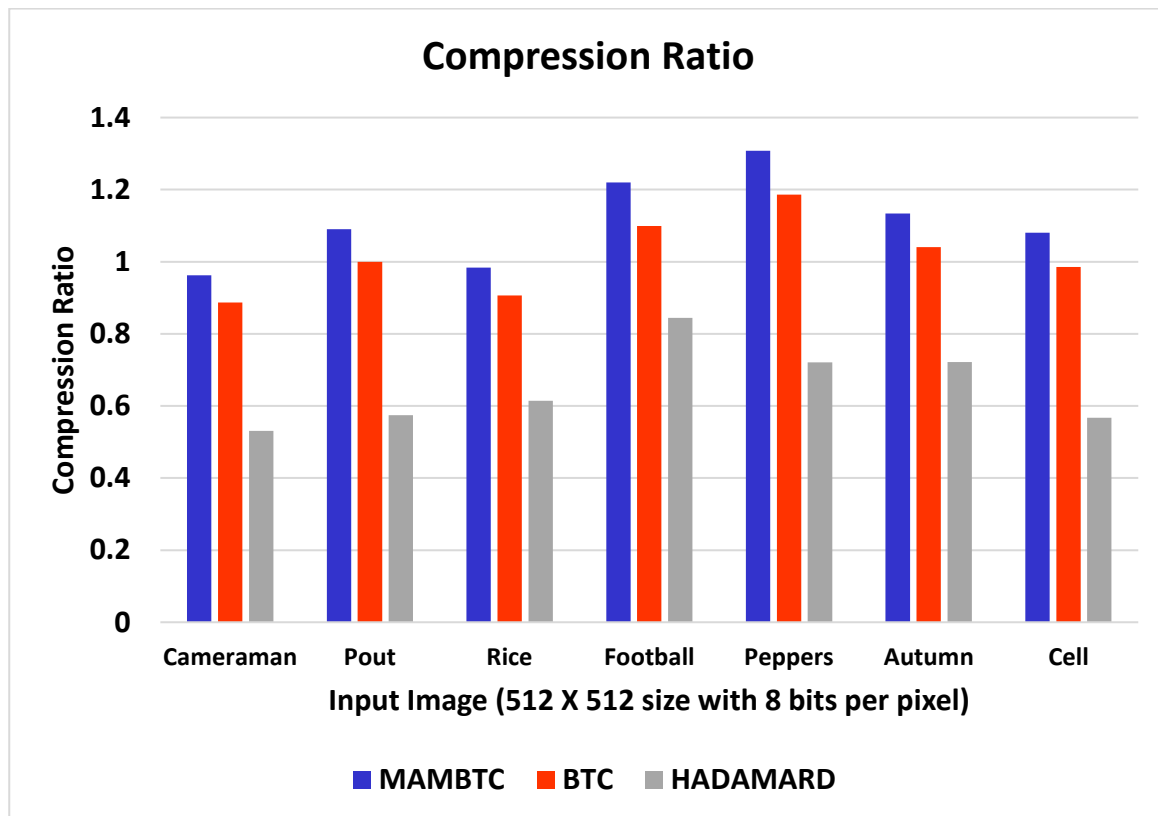
205 4.2 Compression Ratio (CR)

206 The CR is used to determine the compression algorithm performance [17]. Here, the
 207 CR ratio is used to evaluate the MAMBTC compression algorithm. It is the ratio of the
 208 uncompressed image (or) original image file size to the compressed image file size.

209 The compression ratio can be computed by using the formula as:

$$210 \quad \text{Compression Ratio} = \frac{\text{file size of the uncompressed image}}{\text{file size of compressed image}} \quad (9)$$

211 The comparison values of compression ratio among MAMBTC, BTC, and Hadamard
 212 transform techniques are shown in Fig.8 for various input images.



213 **Fig. 8** Comparison of Compression ratio between MAMBTC, BTC, and Hadamard transform techniques for
 214 different Images
 215

216 4.3 Bit Rate (BR)

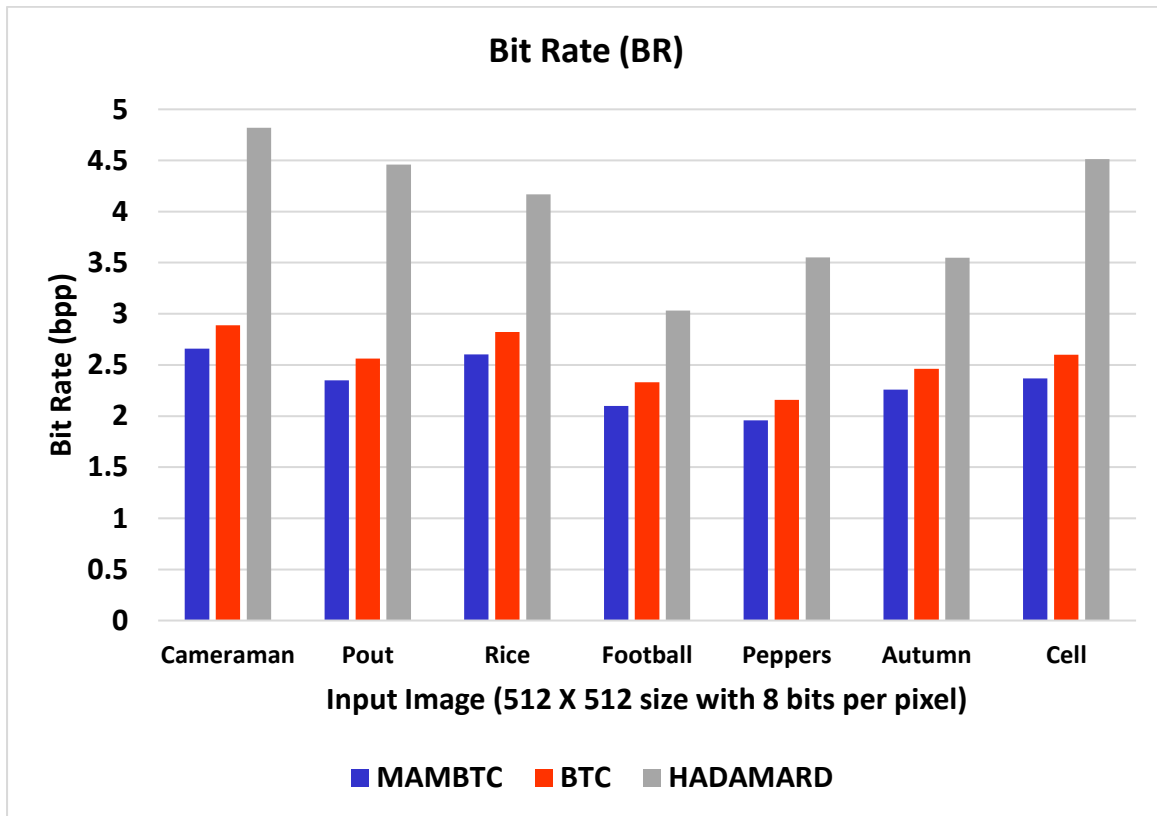
217 Bit rate [17] is also used to determine the compression algorithm performance. The
 218 lower bit rate represents better compression algorithm performance.

219 The bit rate can be computed by using the formula as:

$$220 \quad \text{bit rate} = \frac{b}{\text{compression ratio}} \quad (10)$$

222 Where b is the number of bits per pixel of the uncompressed image. The comparison values of
 223 bit rates among MAMBTC, BTC and Hadamard transform techniques are shown in Fig.9 for
 224 various input images.

225



226

227

228

Fig. 9 Comparison of Bit Rates between MAMBTC, BTC, and Hadamard transform techniques for different Images

229 4.4 Mean Squared Error (MSE)

230 The MSE is used to determine the loss of energy value in lossy compression of the
 231 original value [17]. It is measured by differences in individual pixel's gray values. If the mean
 232 squared error is small, it means that the reconstructed image will be equivalent to the original
 233 image.

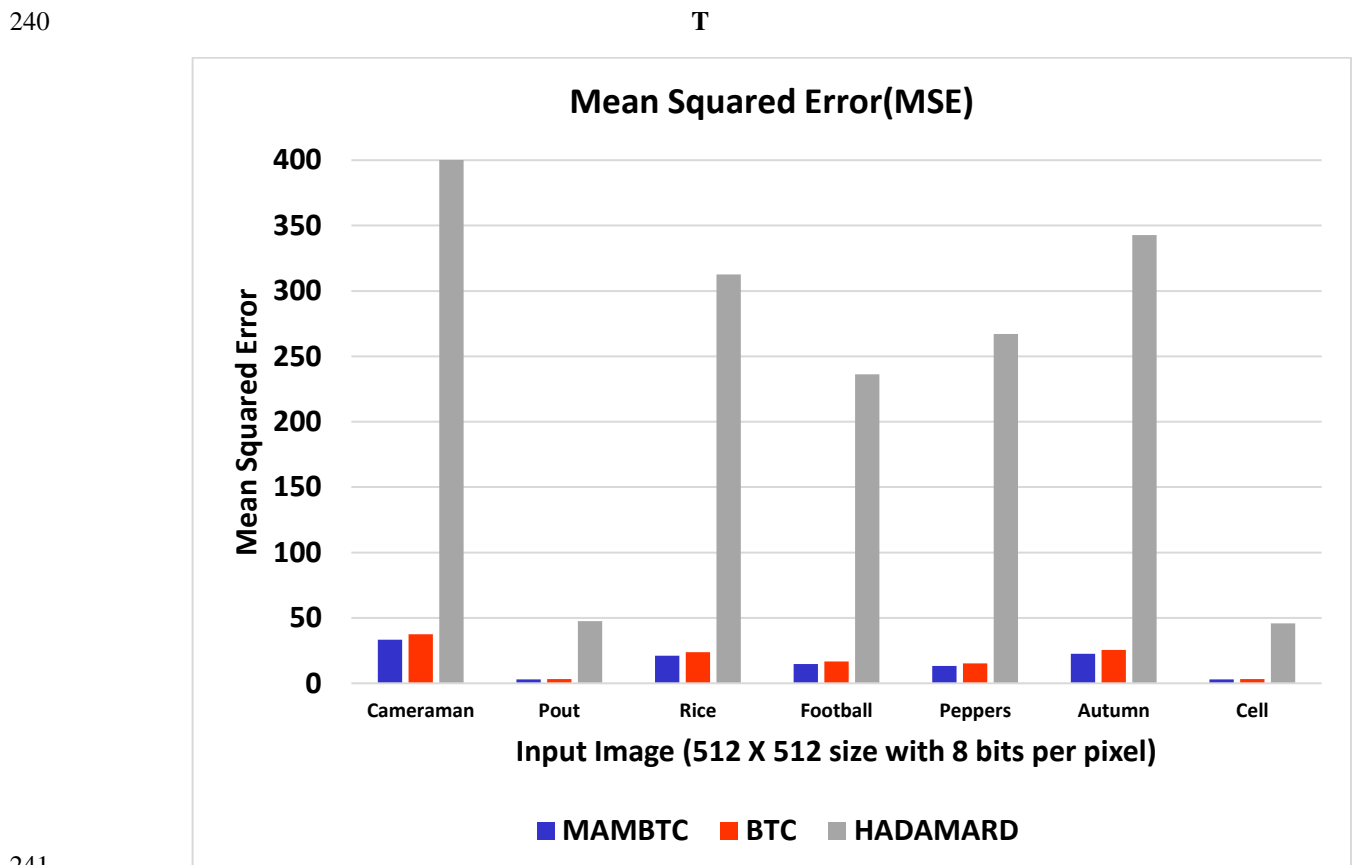
234 Mean Squared Error (MSE) can be computed by using the formula as:

235

$$MSE = \frac{1}{mn} \sum_{i=1}^m \sum_{j=1}^n [out(i,j) - inp(i,j)]^2 \quad (11)$$

236 Where $out(i, j)$ is the compressed image, $inp(i, j)$ is the original image, m and n are the sizes
 237 of rows and columns in the compressed image and original image, respectively.

238 The comparison values of Mean Squared Error (MSE) among MAMBTC, BTC, and
 239 Hadamard transform techniques are shown in Fig.10 for various input images.



241
 242 **Fig. 10** Comparison of MSE between MAMBTC, BTC, and Hadamard transform techniques for
 243 different Images
 244
 245

246 4.5 Weighted Mean Squared Error ($wMSE$)

247 $wMSE$ determines the distortion level in the image. $wMSE$ is based on a correlation
 248 between neighboring pixels since it has different effects on the human visual system when
 249 pixels are at different positions in an image [17].

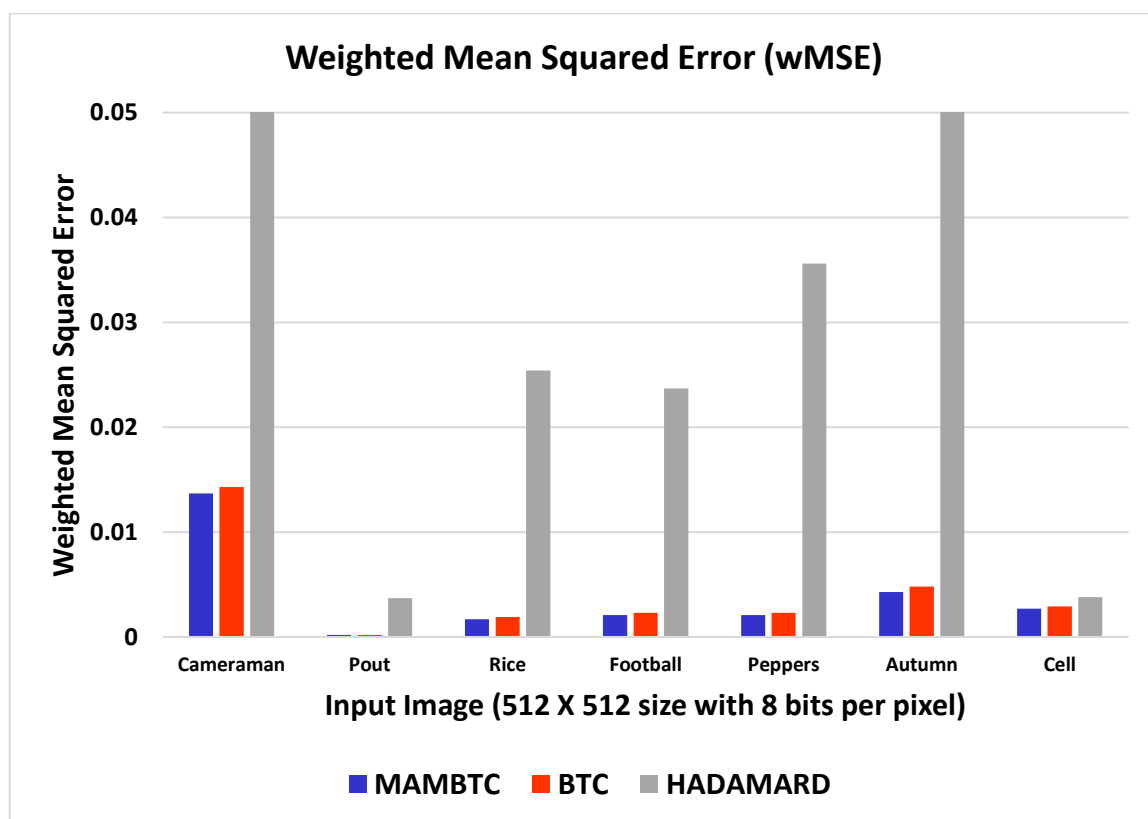
250 Weighted Mean Squared Error ($wMSE$) can be computed by using the formula as:

$$wMSE = \frac{1}{mn} \sum_{i=1}^m \sum_{j=1}^n \left(2 \left| \frac{out(i,j) - inp(i,j)}{out(i,j) + inp(i,j)} \right| \right)^2 \quad (12)$$

Where, $out(i, j)$ is the compressed image, $inp(i, j)$ is the original image, m and n are the sizes of rows and columns in the compressed image and original image, respectively.

The comparison values of $wMSE$ among MAMBTC, BTC, and Hadamard transform techniques are shown in Fig.11 for various input images.

256



257

258

259

Fig. 11 Comparison of $wMSE$ between MAMBTC, BTC, and Hadamard transform techniques for different Images

260 4.6 Peak Signal to Noise Ratio (PSNR)

261 The PSNR is a metric used for qualitative measurement of reconstructed image for lossy
 262 compression [22], [23]. The reconstructed image quality will be better if a higher PSNR value
 263 is obtained.

264 PSNR can be computed by using the formula as:

$$PSNR = 10 \log_{10} \frac{255^2}{MSE} \quad (13)$$

Where MSE is the mean squared error.

The comparison values of PSNR among MAMBTC, BTC and Hadamard transform techniques are shown in Fig.12 for various input images.

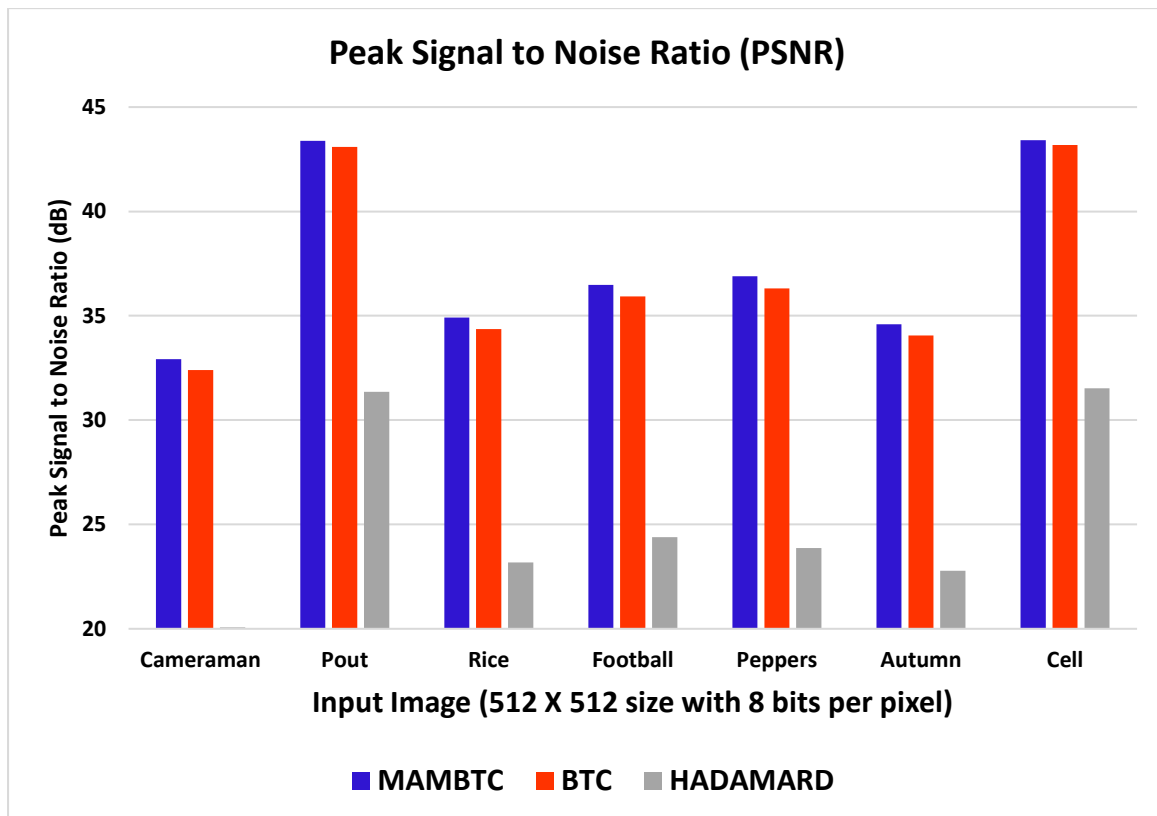


Fig. 12 Comparison of PSNR between MAMBTC, BTC and Hadamard transform techniques for different Images

4.7 Weighted Peak Signal to Noise Ratio (*wPSNR*)

The *wPSNR* [17] is an extension of PSNR. The measurement of *wPSNR* is based on neighboring pixels and the human visual system. The *wPSNR* gives the image quality and is calculated between original and compressed content.

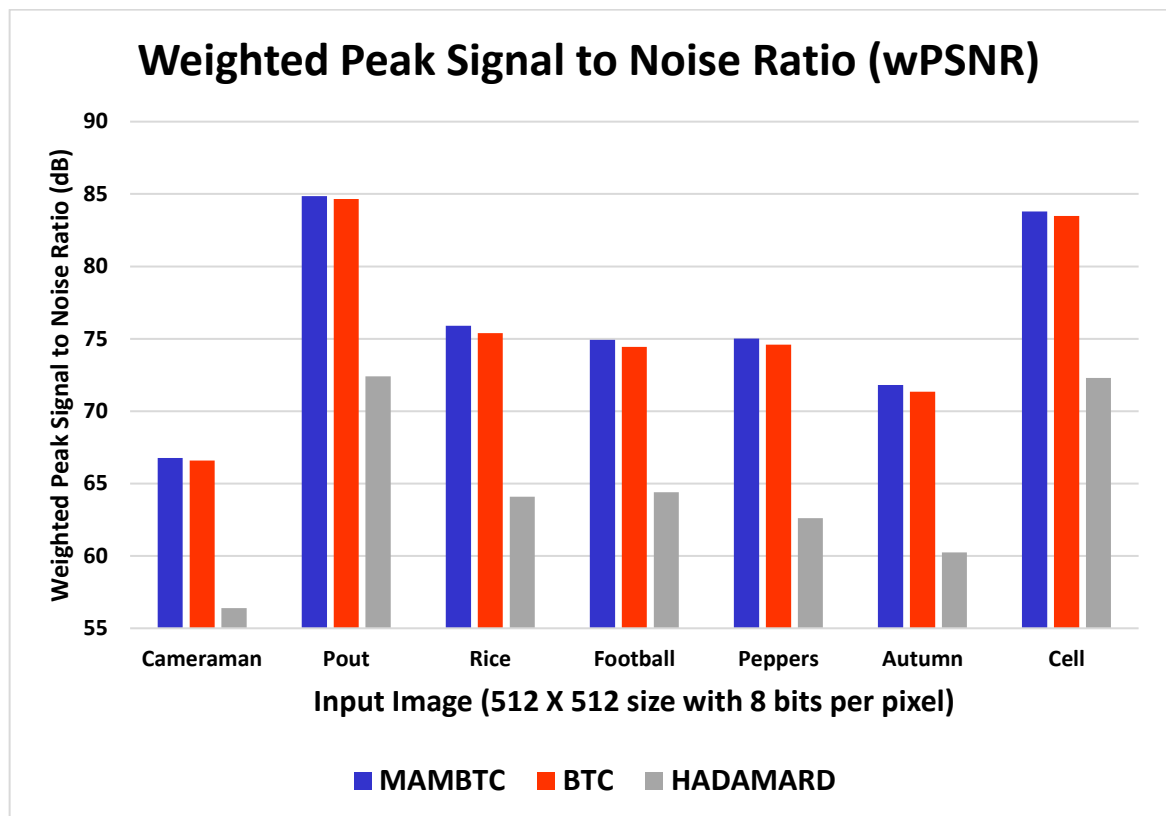
wPSNR can be computed by using the formula:

$$wPSNR = 10 \log_{10} \left(\frac{255^2}{wMSE} \right) \quad (14)$$

278 Where wMSE is a weighted mean squared error.

279 The comparison values of wPSNR between MAMBTC, BTC and Hadamard transform
 280 techniques are shown in Fig.13 for various input images.

281



282

283

284

Fig. 13 Comparison of wPSNR between MAMBTC, BTC and Hadamard transform techniques for different Images

285 4.8 Computational Time

286 The comparison values of computational time [24] among MAMBTC, BTC and
 287 Hadamard transform techniques are shown in Fig.14 for various input images. Even though
 288 MAMBTC has higher computational complexity than BTC, but the compression ratio of
 289 MAMBTC is better than BTC.

290

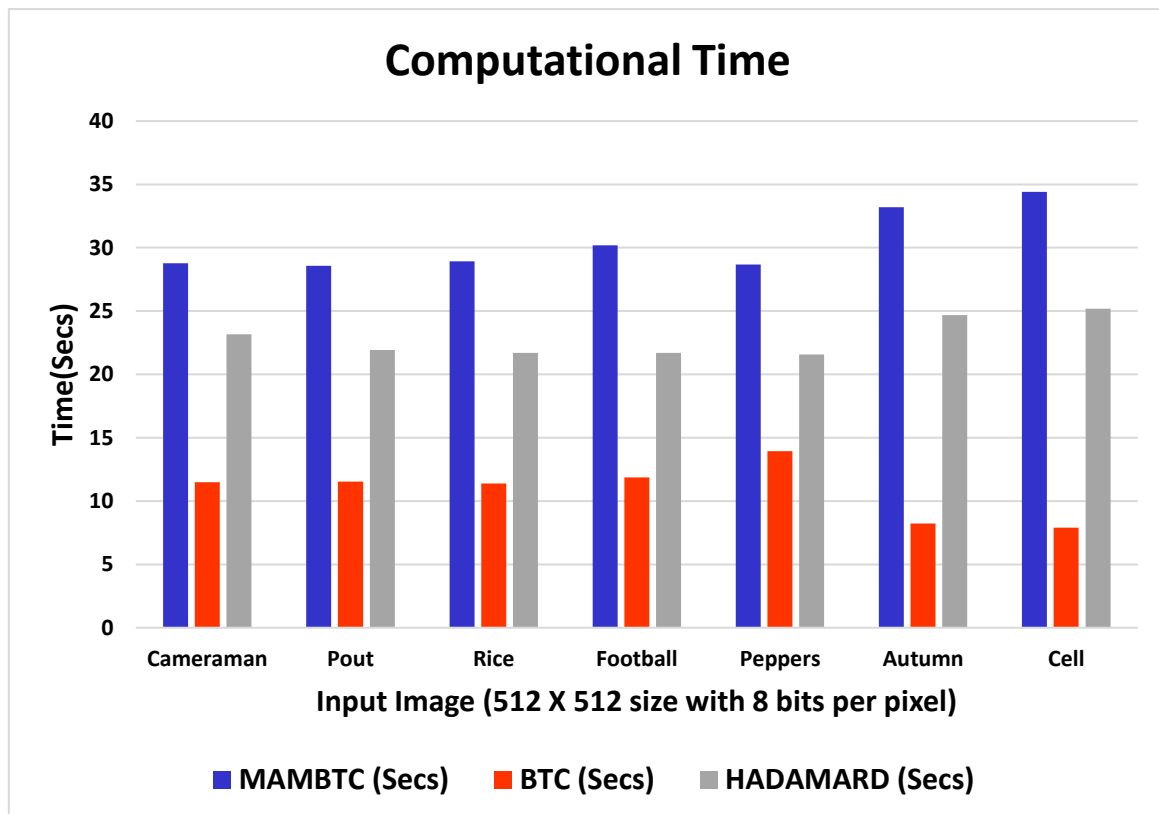


Fig. 14 Comparison of Computation Time between MAMBTC, BTC and Hadamard transform techniques for different Images

291
292
293

294 4.9 Memory Size

295 The comparison values of memory size [24] among MAMBTC, BTC and Hadamard
296 transform techniques are shown in Fig.15 for various input images. Fig. 15 infers that the
297 MAMBTC requires lesser memory than the BTC and Hadamard techniques for compressing
298 the different standard input images.

299 Table 1 lists the performance evaluation of proposed system values such as
300 Compression Ratio, Bit Rate, MSE, wMSE, PSNR, wPSNR, Computational Time and Memory
301 Size.

302

303

304

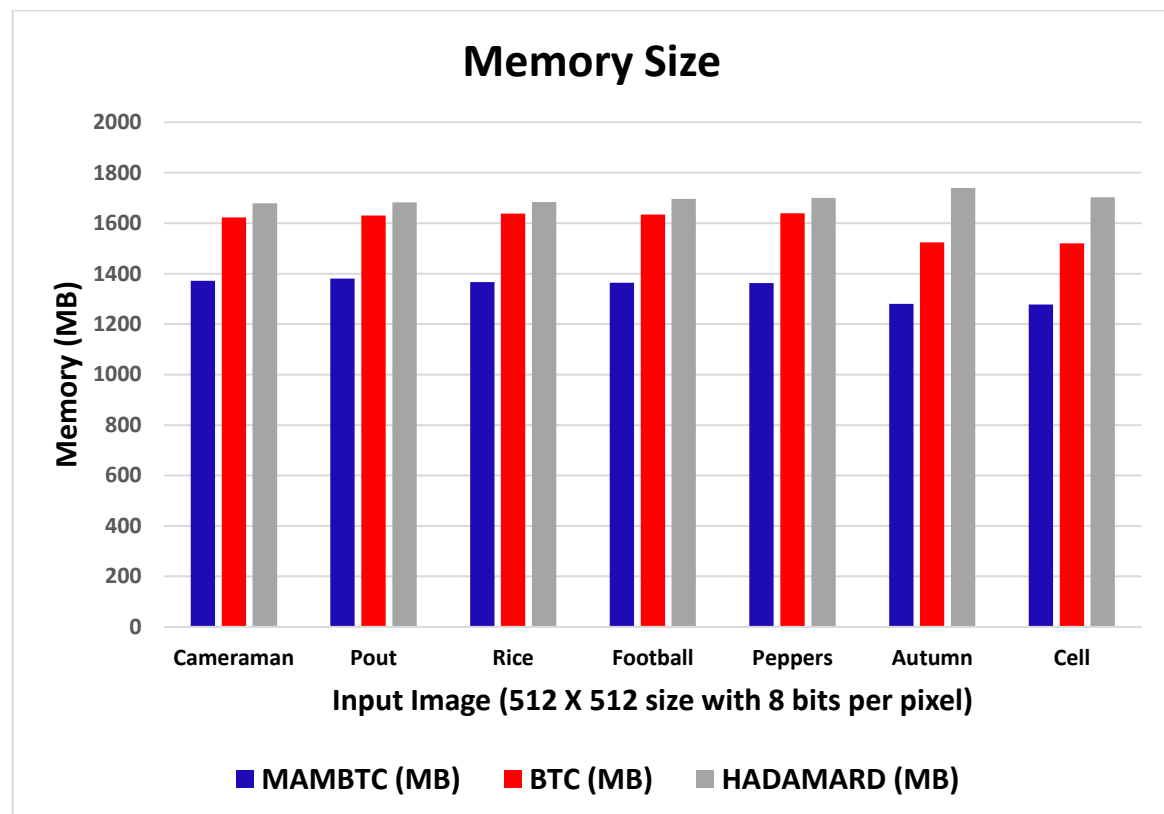
305

Table 1 Performance Evaluation of Proposed System

Input Image	Compression Ratio	Bit Rate	MSE	wMSE	PSNR (dB)	wPSNR (dB)	Computational Time (Secs)	Memory Size (MB)
Cameraman	0.9623	2.6603	33.2453	0.0137	32.9135	66.7728	28.772	1371
Pout	1.0901	2.3483	2.9861	0.0002	43.3797	84.8556	28.5758	1380
Rice	0.9839	2.6019	20.9969	0.0017	34.9093	75.898	28.9336	1367
Football	1.2201	2.0981	14.624	0.0021	36.4801	74.9267	30.199	1364
Peppers	1.3077	1.9576	13.2815	0.0021	36.8983	75.0046	28.6825	1363
Autumn	1.1342	2.2571	22.5541	0.0043	34.6005	71.8069	33.1961	1280
Cell	1.0808	2.3686	2.9595	0.0027	43.4187	83.7846	34.4036	1278

306

307



308

309

310

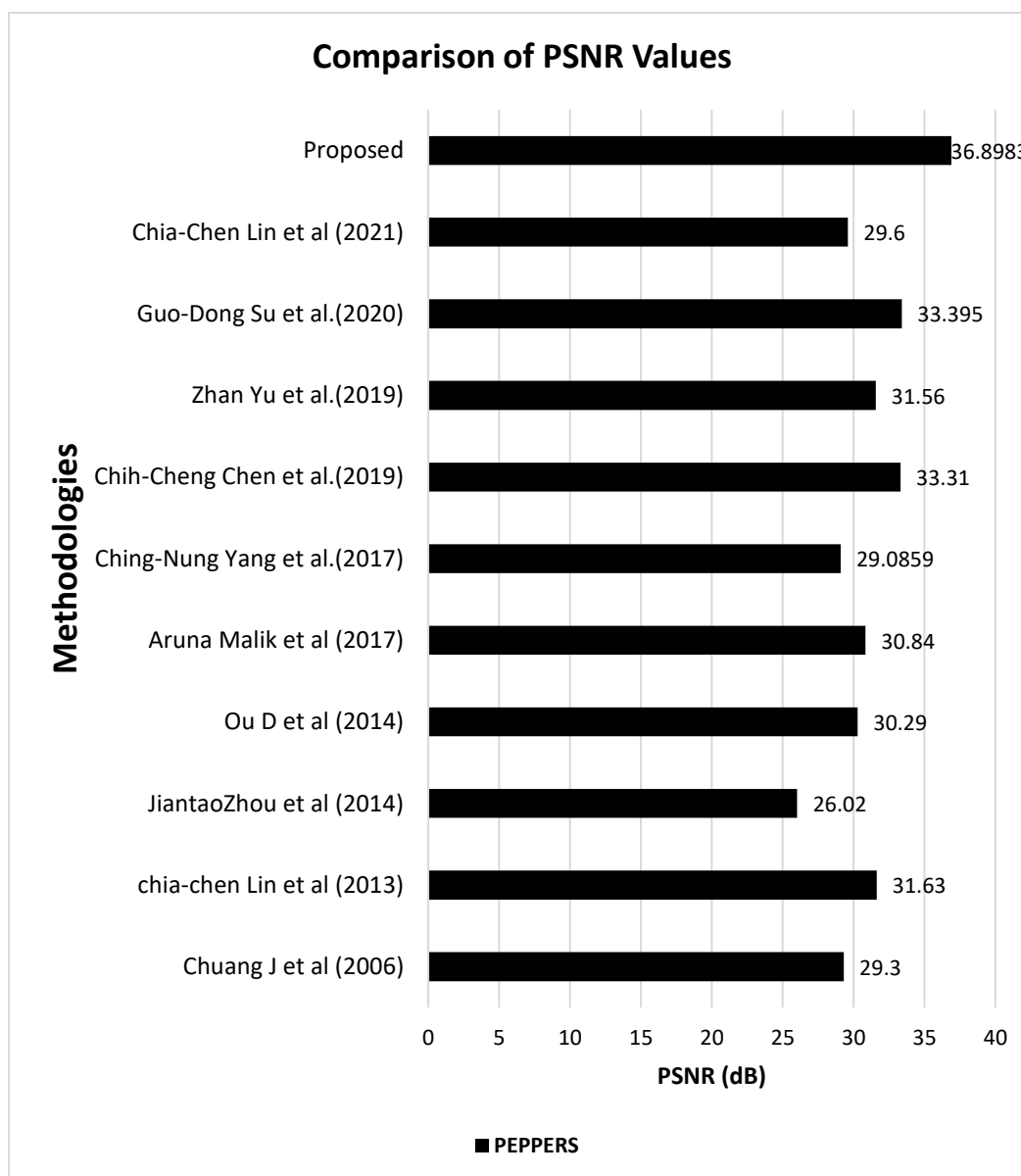
Fig. 15 Comparison of Memory Size between MAMBTC, BTC and Hadamard transform techniques for different Images

311

312

313

Figure 16 compares the various state of the art techniques with the present proposed system by comparing the PSNR values with Pepper image. The resultant graph shows that the proposed system of this study is much better than the various state of the art techniques.



314
315

Fig. 16 Comparison between various state of art techniques with the proposed system

316 5. Conclusion

317 In this paper, the researchers have presented a novel scheme of scalable coding of
 318 encryption of images using the MAMBTC. The original input image is compressed by using
 319 the MAMBTC. Then using PRNG, it is encrypted, and the encoded bit-stream is transmitted.
 320 The original image is reconstructed by the MAMBTC, which is further scaled by scaling factor
 321 2 and bilinear interpolation technique at the decoder. It requires low storage, and coding and
 322 decoding techniques of MAMBTC are simpler. The requirement for computational complexity
 323 is higher for MAMBTC since it needs both the high range and low range values of each non-

324 overlapping block, but the compression ratio is higher than BTC, and the requirement for
 325 storage space is decreased when compared to BTC. The experiment results show that it has
 326 improved performance than BTC with increased PSNR, increased compression ratio, increased
 327 wPSNR, decreased MSE, decreased wMSE, and decreased bit rate. As a result, the proposed
 328 method is very robust and effective for Signal Processing Community to transmit signals on
 329 encrypted domains than the existing techniques available.

330 List of abbreviations

331 Table 2 shows the various abbreviations used in this paper

332 **Table 2** Utilized parameter and their functionality

S.No	Parameters	Working outcomes of the parameters
1	X_{HV}	Higher range value of the non-overlapping block
2	X_{LV}	Lower range value of the non-overlapping block
3	\bar{x}	Mean value of the non-overlapping block
4	$c(i, j)$	Binary Block of the non-overlapping block of an encoder
5	$pr(i, j)$	The pseudo-random generated value
6	$en(i, j)$	Encrypted Pixel Value
7	$de(i, j)$	Decrypted Pixel Value
8	$re(i, j)$	Reconstructed Pixel Value
9	MSE	Mean Squared Error Value
10	wMSE	Weighted Mean Squared Error Value
11	PSNR	Peak Signal to Noise Ratio
12	wPSNR	Weighted Peak Signal to Noise Ratio
13	CR	Compression Ratio
14	BR	Bit Rate
15	PRNG	Pseudo-random number generated value
16	SSP	Secured Signal Processing

333 Declarations

334 Availability of data and materials

335 The conclusion and comparison data of this article are included within the article

336 Competing Interests

337 The authors declare that they have no competing interests

338 **Funding**

339 Not Applicable

340 **Author's Contributions**

341 JBP proposed the framework of this work and carried out the whole experiments and drafted
342 the manuscript. VG greatly helped in articulating the manuscript. YZ helped in finalizing the
343 manuscript. MPR, AM and AT have helped in technical writing. All authors read and approved
344 the final manuscript.

345 **Acknowledgements**

346 Not Applicable

347 **References**

- 348 1. Z.Erkin et al., Protection and retrieval of encrypted multimedia content: When cryptography
349 meets signal processing. *EURASIP Journal on Information Security*. **2007**, 1-20 (2007).
350 doi:10.1155/2007/78943.
- 351 2. T.Bianchi et al., On the implementation of the discrete Fourier transform in the encrypted
352 domain. *IEEE Transformation on Information Forensics and Security*. **4**(1), 86–97 (2009).
353 doi:10.1109/tifs.2008.2011087.
- 354 3. J.R.Troncoso Pastoriza, F.Pérez-González, Secure adaptive filtering. *IEEE Transformation*
355 *on Information Forensics and Security*. **6**(2),469–485(2011).
356 doi:10.1109/tifs.2011.2109385.
- 357 4. T.Bianchi et al., Composite signal representation for fast and storage-efficient processing of
358 encrypted signals. *IEEE Transformation on Information Forensics and Security*. **5**(1),180–
359 187 (2010). doi:10.1109/tifs.2009.2036230.
- 360 5 N.Memon, P.W.Wong, A buyer-seller watermarking protocol. *IEEE Transactions on Image*
361 *Processing*. **10**(4), 643–649 (2001). doi:10.1109/83.913598.

- 362 6. M.Kuribayashi, H.Tanaka, Fingerprinting protocol for images based on an additive
363 homomorphic property. *IEEE Transactions on Image Processing*. **14**(12), 2129–2139
364 (2005). doi:10.1109/tip.2005.859383.
- 365 7. M.Johnson et al., On compressing encrypted data. *IEEE Transactions on Signal Processing*.
366 **52**(10), 2992–3006 (2004). doi:10.1109/tsp.2004.833860.
- 367 8. D.Schonberg et al., On blind compression of encrypted correlated data approaching the
368 source entropy rate. in 43rd Annual Allerton Conference, Allerton, IL, USA (2005).
- 369 9. R.Lazzeretti, M.Barni, Lossless compression of encrypted grey level and color images. in
370 16th European Signal Processing Conference, pp. 1-5, Lausanne, Switzerland (2008)
- 371 10. A.Kumar, A.Makur, Lossy compression of encrypted image by Compressing sensing
372 technique. in *IEEE Region 10 Conference (TENCON2009)*, pp.1–6 (2009).
373 doi:10.1109/TENCON.2009.5395999.
- 374 11. X.Zhang, Lossy compression and iterative reconstruction for encrypted image. *IEEE*
375 *Transformation on Information Forensics and Security*. **6**(1), 53–58 (2011).
376 doi:10.1109/tifs.2010.2099114.
- 377 12. A.Bilgin et al., Scalable image coding using reversible integer wavelet transforms. *IEEE*
378 *Transactions on Image Processing*. **9**(11), 1972–1977 (2000). doi:org/10.1109/83.877218.
- 379 13. D.Taubman, High performance scalable image compression with EBCOT. *IEEE*
380 *Transactions on Image Processing*. **9**(7),1158–1170 (2000). doi:org/10.1109/83.847830.
- 381 14. Zhang Xinpeng et al., Scalable Coding of Encrypted Images. *IEEE Transactions on Image*
382 *Processing*. **21**(6),3108-3114. doi:org/10.1109/TIP.2012.2187671.
- 383 15. Edward J. Delp, O. Robert Mitchell, Image Coding Using Block Truncation Coding. *IEEE*
384 *Transactions on Communications*, **27**, 1335-1342, (1979).
385 doi:org/10.1109/TCOM.1979.1094560.

- 386 16. M.D.Lema, O.R.Mitchell, Absolute Moment Block Truncation Coding and its Application
387 to color images. *IEEE Transactions on Communications*. **32**(10),1148-1157, (1984).
388 doi:org/10.1109/TCOM.1984.1095973.
- 389 17. P.Jeya Bright, G.Vishnuvarthanan, Development of a scalable coding for the encryption of
390 Images using Block Truncation Code, in 3rd International Conference on Trends in
391 Electronics and Informatics (ICOEI 2019), pp.934-938, Tirunelveli, India, (2019).
392 doi:org/10.1109/ICOEI.2019.8862525.
- 393 18. Ching-Nung Yang et al., Constructions of general (k,n) reversible AMBTC based visual
394 cryptography with two decryption options. *Journal of Visual Communication and Image*
395 *Representation*. **48**,182-194, (2017). doi:org/10.1016/j.jvcir.2017.06.012.
- 396 19. Guo-Dong Su, Chin-Chin Chang, A High Capacity Reversible Data Hiding in Encrypted
397 AMBTC-Compressed Images. *IEEE Access*. **8**, 26984–27000, (2020).
398 doi:org/10.1109/ACCESS.2020.2966234.
- 399 20. Chih-Cheng Chen et al., TSIA: A Novel Image Authentication Scheme for AMBTC-Based
400 Compressed Images Using Turtle Shell Based Reference Matrix. *IEEE Access*. **7**,149515-
401 149526, (2019). doi:org/10.1109/ ACCESS.2019.2944833.
- 402 21. Zhan Yu et al., HBF-DH: An Enhanced Payload Hybrid Data Hiding Method Based on a
403 Hybrid Strategy and Block Features. *IEEE Access*. **7**, 148439–148452, (2019).
404 doi:org/10.1109/ACCESS.2019. 2943505.
- 405 22. Stephen.T.Welstead, *Fractal and Wavelet Image Compression Techniques*, pp.155-156,
406 SPIE Publication, Washington (1999)
- 407 23. Raouf Hamzaoui and Dietmar Saupe, *Fractal Image Compression-Document and Image*
408 *Compression*, pp.168-169, CRC Press (2006)
- 409 24. Saravanan Alagarsamy et al., Multi-channeled MR brain image segmentation: A new
410 automated approach combining BAT and clustering technique for better identification of

- 411 heterogeneous tumors. *Biocybernetics and Biomedical Engineering*. **39**(4), 1005-1035,
412 (2019). doi:org/10.1016/j.bbe.2019.05.007.
- 413 25. J.C.Chuang, C.C Chang, Using a simple and fast image compression algorithm to hide
414 secret information. *International Journal of Computers and Applications*. **28**(4),329–333,
415 (2006). doi:org/10.1080/1206212X.2006.11441818.
- 416 26. Duanhao Ou, Wei Sun., High payload image steganography with minimum distortion based
417 on absolute moment block truncation coding. *Multimedia Tools Appl*. **74**, 9117–9139,
418 (2014). doi:org/10.1007/s11042-014-2059-2.
- 419 27. Aruna Malik et al., A high payload data hiding scheme based on modified AMBTC
420 technique. *Multimedia Tools Appl*. **76**,14151–14167, (2017). doi:org/10.1007/s11042-
421 016-3815-2.
- 422 28. Jiantao Zhou et al., Scalable Compression of Stream Cipher Encrypted Images Through
423 Context-Adaptive Sampling. *IEEE Transactions on Information Forensics and Security*.
424 **9**(11),1857–1868, (2014). doi.org/10.1109/TIFS.2014.2352455.
- 425 29. Chia-Chen Lin et al., A Novel Reversible Data Hiding Scheme Based on AMBTC
426 Compression Technique. *Multimedia Tools Appl*, **74**, 3823–3842,(2013).
427 doi:org/10.1007/s11042-013-1801-5.
- 428 30. Chia-Chen Lin et al., Reversible Data Hiding for AMBTC Compressed Images Based on
429 Matrix and Hamming Coding. *MDPI-Electronics*. **10**(281), 1-20, (2021).
430 doi:org/10.3390/electronics10030281.

